Sharif University of Technology

Scientia Iranica

Transactions on Civil Engineering

https://scientiairanica.sharif.edu

Estimation of the effective moment of inertia for hybrid concrete beams reinforced with steel and FRP bars

Fahimeh Maleki, Ali Kheyroddin, Hosein Naderpour, Masoomeh Mirrashid *

Faculty of Civil Engineering, Semnan University, Semnan, Iran Iran.

* Corresponding author: m.mirrashid@semnan.ac.ir (M. Mirrashid)

Received 4 March 2022; received in revised form 17 November 2022; accepted 21 February 2023

Keywords

Artificial Neural Networks (ANN);
Adaptive Neural Fuzzy Inference System (ANFIS);
Effective moment of inertia;
Hybrid concrete beam;
Fiber-Reinforced Polymer (FRP) bars.

Abstract

The application of fiber-reinforced polymer bars is rapidly rising in concrete structures because of corrosion resistance and high tensile strength. By contrast, concrete structures reinforced with Fiber-Reinforced Polymer (FRP) bars illustrate less ductility and brittle failure without warning than Reinforced Concrete (RC) structures with conventional steel bars. Hybrid concrete structures with the combination of FRP and steel bars can simultaneously increase strength and ductility. This paper aims to estimate the effective moment of inertia in hybrid concrete beams by using a neuro-fuzzy technique and Artificial Neural Networks (ANN). A new equation has been proposed for hybrid beams with attention to the importance of calculating the effective moment of inertia in concrete beams. The proposed equation has been considered the effect of elastic modulus and hybrid reinforcement ratio on this parameter for hybrid RC beams having FRP bars. This equation has been presented based on the Neural Networks (NNs) and experimental data conducted by other researchers on the simple beams to calculate the effective moment of inertia for hybrid RC beams. The result shows that both Soft Computing (SC) models are highly precise compared to experimental data.

1. Introduction

During recent decades, the corrosion of steel bars in Reinforced Concrete (RC) structures exposed to deicing salts and marine environments has become a significant concern. To avoid deterioration in this condition, the use of Fiber-Reinforced Polymer (FRP) bars increased because of their high strength-to-weight ratios, corrosion resistance compared to conventional steel bars, durability, and non-magnetic. However, because of linear elastic behavior up to the failure of FRP bars, concrete structure members reinforced with this reinforcement exhibit more significant crack widths and deflection than steel-RC members [1]. Therefore, researchers a combination of FRP and steel bars suggested as an effective solution in concrete elements to solve these problems [2]. Using the additional steel bars can increase the flexural members' ductile behavior in hybrid RC members than concrete members reinforced with pure FRP bars. Thus, steel and FRP bars significantly improve ductility and strength in the hybrid beams, respectively. One of the essential factors for providing the balance between improving strength and ductility is the hybrid reinforcement ratio. Qin et al. [3] recommended this ratio within the range of 1 to 2.5 in the over-reinforcement hybrid beams. The study by Akiel et al. [4] showed that members reinforced with hybrid steel-BFRP bars have less deflection and smaller crack widths under service conditions than RC members having BFRP bars only. Sheik and Kharal [5] evaluated the behavior of Glass Fiber Reinforced Polymer (GFRP)-RC beams in flexural, shear, tension, and compression. The results of their studies indicate that the proposed tension-stiffening model is a significantly improves in the prediction

To cite this article:

F. Maleki, A. Kheyroddin, H. Naderpour, M. Mirrashid "Estimation of the effective moment of inertia for hybrid concrete beams reinforced with steel and FRP bars", *Scientia Iranica* (2025) **32**(7): 6576 https://doi.org/10.24200/sci.2023.60066.6576

of deflection and stiffness of the beams. Salleh et al. [6] evaluated the load-deflection behavior, ratio, and the ordinate of GFRP to steel in hybrid RC beams using ATENA software. Pang et al. [7] investigated the appropriate reinforcement ratio limits to ensure sufficient strength and ductility in hybrid FRP-steel RC beams. EL Refai et al. [8] proposed a bond coefficient to estimate the crack width of concrete beams reinforced with hybrid bars base on the ACI-440.1R-06 equation. Kara et al. [9] presented a numerical method using force equilibrium and strain compatibility to predict the curvature, deflection, and moment capacity of hybrid RC beams. Dunder et al. [1] proposed a numerical method to calculate the deflection of hybrid beams regardless of the reinforcement type. Al-Sunna et al. [10] experimentally evaluated deflection in RC beams and slabs having FRP bars to compare with existing equations. Naderpour et al. [11] investigated a proposed equation using the Artificial Neural Network (ANN) to predict the FRP-confined compressive strength of concrete. Kheyroddin [12] and Bui et al. [13] presented a new equation to determine the effect of tension and compression reinforcement ratio, concrete compressive strength, and the form of loading on the flexural rigidity (EI) of RC beams. Bui et al. [14] investigated the ductility of the hybrid RC beams considering various factors, including the effects of the FRP/steel reinforcement ratio, the location and form of FRP bars, and the concrete compressive strength. Shield et al. [15] performed many experiments to recommend a recalibration of bond-dependent coefficients in concrete elements Reinforced with GFRP bars. Nguyen et al. [16] presented a simple equation for predicting the effective moment of inertia (I_e) for FRP beams using Gene Expression Programming (GEP). Ge et al. [17] investigated the flexural behavior of concrete beams reinforced with steel-FRP composite bars. Moolaei et al. [18] experimentally evaluated the flexural behavior of beams reinforced with GFRP and steel bars and High-Performance Fiber Reinforced Cementitious Composites (HPFRCC). Wang et al. [19] investigated the flexural behavior of five hybrid BFRP and steel bars RC beams subject to four-point bending tests. Arabshahi et al. [20] proposed an equation for the effective moment of inertia in concrete beams reinforced with FRP bars. Lyu et al. [21] studied the usage of back-propagation Neural Network (NN) and Genetic Algorithm (GA) for the predicting of torsional strength RC beams. Li et al. [22] used an artificial NN and an imperialist competitive algorithm to provide an accurate method for simulating the deflection of the RC beam. Jayasinghe et al. [23] using ANN showed that the new equation for the shear strength of the RC beam in ACI 318–19 and AS 3600–2018 is more accurate compared to other provisions. Alagundi and Palanisamy [24] proposed a model of ANN for prediction of shear strength of an exterior beam-column joint. Zayan and Mahmoud [25] stated that the proposed artificial NN can successfully evaluate the combined flexural torsional strength of Prestressed Concrete (PSC) beams. Zhang et al. [26] application Convolutional Neural Networks (CNNs) to recognize the symmetry group and symmetry order in planar structures. Khan et al. [27] used an artificial NN and a random forest to estimate the Flexural Strength of beams. The results of the ANN showed that the bottom flexural bars of the beam are the most effective factor in yielding flexural capacity. Peng et al. [28] proposed the Adaptive Neural Fuzzy Inference System (ANFIS) method to investigate the flexural behavior of corroded concrete beams. Because in the finite element method, many inputs are required that it was expensive to collect this amount of data. Barkhordari et al. [29] showed that the Hybrid Algorithm (PSO-ANN) for computing the shear strength of deep RC beams has high accuracy and used SHapley Additive exPlanations (SHAP) method to exhibit the effective parameters for estimating shear strength beams. In this study, due to the lack of accuracy of the existing equations in calculating the effective moment of inertia in the hybrid RC beams, equations were proposed. Machine learning and numerical studies are widely used to investigate the behavior of beams, columns, and bridges [30-32].

2. Research significance

The short-term deflection is estimated using the effective moment of inertia at the service load [33]. The primary purpose of this study is to investigate the effect of the elastic modulus of FRP and steel bars and hybrid reinforcement ratio, A_f/A_s, on the effective moment of inertia for hybrid RC beams. Besides, existing methods for calculated the effective moment of inertia are not suitable in hybrid beams. Because these equations proposed to calculate the effective moment of inertia in beams reinforced with FRP or steel bars and they do not have enough accuracy in hybrid beams. Consequently, a new model is presented based on an artificial NN, and then this model provides a comparison of experimental data and other present equations.

3. Existing models

Serviceability is defined as satisfactory performance at service load levels that can be described in terms of cracking and deflection criteria. Excessive deflection is undesirable for the appearance and efficiency of the structure. Excessive crack width also seriously affects the aesthetic and durability of the structure [34]. One common and plain method for calculating deflection is the use of I_e. As the cracking load exceeds, flexural stiffness changes due to the existence of discrete cracks along with the member [35]. I_e accounted for considering the effect of the flexural stiffness variation and concrete tension stiffening. The Eq. (1) proposed by Branson [36] is applicable to steel-RC beams at the service loads.

$$I_e = \left(\frac{M_{cr}}{M_a}\right)^3 I_g + \left[1 - \left(\frac{M_{cr}}{M_a}\right)^3\right] I_{cr} \le I_g, \quad (1)$$

where I_g is the gross moment of inertia, I_{cr} is the cracked moment of inertia, M_{cr} and M_a are the cracking moment and applied moments at the critical section, respectively.

The results of studies provide reveal that this equation overestimates I_e in concrete beams reinforced with FRP bars, especially in beams are under reinforcement [37-40].

Bischoff [41] suggested an equation for I_e, which could be computed from Eqs. (2) and (3). This equation compared with experimental results illustrates that is suitable for both steel and FRP RC beams:

$$I_e = \frac{I_{cr}}{1-\eta\left(M_{cr}/M_a\right)^2} \le I_g , \tag{2}$$

$$\eta = 1 - \frac{I_{cr}}{I_g} . \tag{3}$$

The ACI 440.1R-15 [34] committee offered an additional factor γ, in the equation proposed by Bischoff to consider the variety in stiffness along the length of the member, as illustrated in Eq. (4). The new expression presents a reasonable approximation of the deflection for RC beams with FRP and one-way slabs [42].

$$I_e = \frac{I_{cr}}{1-\gamma\left(\frac{M_{cr}}{M_a}\right)^2\left[1-\frac{I_{cr}}{I_g}\right]} \le I_g \quad \text{where} \quad M_a \ge M_{cr} . \tag{4}$$

The factor γ is defined based on the load and boundary conditions and considers the length of the uncracked regions of the element and change in stiffness in the crack regions [34]. This factor could be computed from Eq. (5).

$$\gamma = 1.72 - 0.72\left(M_{cr}/M_a\right) . \tag{5}$$

Benmokrane et al. recommended Eq. (6), which calibrated utilizing a few numbers of experimental data [37].

$$I_e = \alpha I_{cr} + \left(\frac{I_g}{\beta} - \alpha I_{cr}\right)\left[\frac{M_{cr}}{M_a}\right]^3 . \tag{6}$$

The factor α which exhibiting the diminished composite behavior between the FRP bars and concrete is equal to 0.84. The factor β is equal to 7, which was applied to provide a faster transition from I_g to I_{cr}.

Pirayeh Gar et al. [35] have proposed an equation to predict the deflection of FRP, PSC beams regardless of the I_{cr}/I_g ratio.

Mousavi and Esfahani [43] evaluated the effect of several parameters on the power m in the equation of Branson utilizing the GA method. The proposed equations for I_e can be determined as follows:

The objective function of model A has been described by Eq. (7):

$$e = \left|\delta_{\exp} - \delta_{cal}\right| . \tag{7}$$

Model A is described by Eqs. (8) and (9) as follows.

$$\left(I_e\right)_{Model\ A} = 0.15\left(\frac{M_{cr}}{M_a}\right)^m I_g + 0.89\left[1-\left(\frac{M_{cr}}{M_a}\right)^m\right] I_{cr} \le I_g , \tag{8}$$

$$m = 0.66 - 0.3\frac{\rho_f}{\rho_{fb}} + 1.94\frac{M_{cr}}{M_a} + 4.64\frac{E_f}{E_s} . \tag{9}$$

The objective function of Model B has been described by Eq. (10):

$$e = \left|\left(I_e\right)_{\exp} - \left(I_e\right)_{theo}\right| . \tag{10}$$

Model B is described by Eqs. (11) and (12):

$$\left(I_e\right)_{Model\ B} = 0.17\left(\frac{M_{cr}}{M_a}\right)^m I_g + 0.94\left[1-\left(\frac{M_{cr}}{M_a}\right)^m\right] I_{cr} \le I_g , \tag{11}$$

$$m = 1.69 - 0.51\frac{\rho_f}{\rho_{fb}} + 1.77\frac{M_{cr}}{M_a} + 6.67\frac{E_f}{E_s} , \tag{12}$$

where E_f and E_s are the elastic modulus of FRP and steel bars, respectively. The ρ_f is the FRP reinforcement ratio, and ρ_{fb} is the FRP balance ratio.

In FRP reinforced beams, the balance reinforcement ratio could be calculated by Eq. (13) where the rupture of FRP bars and concrete crushing occur simultaneously.

$$\rho_{fb} = 0.85\beta_1\frac{f_c^{'}}{f_{fu}}\frac{E_f\varepsilon_{cu}}{E_f\varepsilon_{cu}+f_{fu}} , \tag{13}$$

where f_{fu} is the ultimate tensile stress of FRP bars, β_1 considers between 0.85 and 0.65 with attention to concrete strength, $f_c^{'}$ and ε_{cu} are the concrete compressive strength and maximum concrete compressive strain, respectively.

Kheyroddin and Maleki [44] suggested an equation for calculating I_e in hybrid RC beams using the GA method and experimental data, the proposed expression presented in Eqs. (14) and (15).

$$\left(I_e\right)_{theo} = 0.136\left(\frac{M_{cr}}{M_a}\right)^m I_g + 1.117\left[1-\left(\frac{M_{cr}}{M_a}\right)^m\right] I_{cr} , \tag{14}$$

$$m = 0.836\frac{E_f}{E_s} + 0.208\rho_{fb}\frac{A_f}{A_s} + 3.709\frac{M_{cr}}{M_a} . \tag{15}$$

4. Soft Computing (SC)

The SC method which was first introduced by Zadeh [45], mimics the ability of the human brain and how it relates to the environment of uncertainty and inaccuracy. SC aims to use human knowledge to solve complex problems with acceptable precision to have high similarity with human decision making [46]. Methods in SC were inspired by nature and has been considered as a main technique in structural engineering fields [47-52]. One of the most important reasons for the importance of SC and intelligence Computation is the existence of uncertainties and ambiguities in the real world. The purpose of combining the methods of GA, fuzzy system, and NN in SC is to achieve the ability to solve problems that each method can't solve alone.

Table 1. Experimental studies of hybrid steel/FRP RC beams.

Reference	Number of beam specimens	Number of data	Type of FRP bar
Aiello and Ombres [56]	4	29	AFRP [a]
Qu et al. [57]	6	46	GFRP [b]
Leung and Balendran [58]	4	6	GFRP
Almusallam et al. [59]	2	3	GFRP
Safan [60]	4	4	GFRP
Yang et al. [61]	1	1	GFRP
Refai et al. [8]	6	33	GFRP

[a] **AFRP:** Aramid Fiber Reinforced Polymer; [b] **GFRP:** Glass Fiber Reinforced Polymer

Table 2. Properties of the experimental data.

Parameter	I_g (mm^4)	A_f/A_s	M_{cr}/M_a	E_f/E_s	I_{cr} (mm^4)	ρ_{fb}	$I_{e\text{-}exp}$ (mm^4)
Mean	2.71E+8	1.18	0.44	0.23	6.86E+7	0.0036	8.8E+7
Minimum	6.67E+7	0.25	0.11	0.19	1.57E+7	0.0013	1.25E+7
Maximum	5.18E+8	2.88	0.99	0.73	1.62E+8	0.0073	3.35E+8
Standard deviation	1.66E+8	0.66	0.19	0.05	4.46E+7	0.00134	6.93E+7
Coefficient of variation	0.612	0.564	0.429	0.219	0.65	0.372	0.788

Table 3. Scaling equation for parameters.

Parameter	Scaling equation
I_g (mm^4)	$I_{g\text{-}s} = (0.8) \times (I_g - I_{g\text{-}min})/(I_{g\text{-}max} - I_{g\text{-}min}) + 0.1$
A_f/A_s	$(A_f/A_s)_s = (0.8) \times ((A_f/A_s) - (A_f/A_s)_{min})/((A_f/A_s)_{max} - (A_f/A_s)_{min}) + 0.1$
M_{cr}/M_a	$(M_{cr}/M_a)_s = (0.8) \times ((M_{cr}/M_a) - (M_{cr}/M_a)_{min})/((M_{cr}/M_a)_{max} - (M_{cr}/M_a)_{min}) + 0.1$
E_f/E_s	$(E_f/E_s)_s = (0.8) \times ((E_f/E_s) - (E_f/E_s)_{min})/((E_f/E_s)_{max} - (E_f/E_s)_{min}) + 0.1$
I_{cr} (mm^4)	$I_{cr\text{-}s} = (0.8) \times (I_{cr} - I_{cr\text{-}min})/(I_{cr\text{-}max} - I_{cr\text{-}min}) + 0.1$
ρ_{fb}	$\rho_{fb\text{-}s} = (0.8) \times (\rho_{fb} - \rho_{fb\text{-}min})/(\rho_{fb\text{-}max} - \rho_{fb\text{-}min}) + 0.1$
$I_{e\text{-}exp}$ (mm^4)	$I_{e\text{-}exp\text{-}s} = (0.8) \times (I_{e\text{-}exp} - I_{e\text{-}exp\text{-}min})/(I_{e\text{-}exp\text{-}max} - I_{e\text{-}exp\text{-}min}) + 0.1$

ANN and fuzzy systems are examples of the most important SC models that are widely used in various sciences. In the last few years, powerful systems called the ANFIS have been used in various sciences. These types of systems, by taking advantage of the training power of NNs and the linguistic advantage of fuzzy systems, have been able to benefit from These two models should be used for process analysis. As one of the common neuro-fuzzy systems, ANFIS was suggested by Jang [53] in 1993. This system uses back-propagation gradient descent and the least-squares methods for the training process.

This study was used as two methods consist of ANN and ANFIS models to determine I_e in hybrid beams. To achieve the desired output, for each method select the best model, and the results are evaluated with the experimental.

5. ANN modeling

The artificial NN is one of the branches of soft-computing which has been used in modeling complex nonlinear systems. In recent years, the artificial NN has been considered a powerful computational method. That solves complex problems and can be applied to simulate, evaluate, and approximate with high accuracy.

For the correct equation of Branson, one hundred twenty-two data as follow have been applied. These data are the number of points on the curve of load-deflection hybrid FRP/steel RC beams with four-point loading. Table 1 presents the detail of the experimental specimens used in this study.

The parameters include reinforcement ratio (A_f/A_s), elastic modulus ratio (E_f/E_s), level of loading (M_{cr}/M_a), the gross moment of inertia (I_g), the balance ratio (ρ_{fb}), and cracked moment of inertia (I_{cr}) used as the six input nodes, the target node was the effective moment of inertia. Two hidden layers were utilized in this ANN modeling, where Log-Sigmoid and Purline were transfer functions, respectively. Normalization /scaling for all data was performed and for this purpose, all data were scaled between 0.1 and 0.9. Tables 2 and 3 presented the values of experimental data and normalization equations, respectively.

In the Levenberg-Marquardt method input and target nodes randomly have distributed into three sets, consist of the train, validate, and test the network. Varying the relative percentages of those three sets could slightly improve the generate method. The regression values and Mean Square Error (MSE) of the networks with the different number of hidden nodes exhibit in Figures 1 and 2, respectively.

Table 4. Details of ANN.

Node	Input weights						Layer weights	Bias to	
	Input 1	Input 2	Input 3	Input 4	Input 5	Input 6		Hidden layer	Output layer
Node 1	1.0586	-1.0264	-1.9345	2.6546	-1.8642	-1.9836	-1.0917	-4.4309	-
Node 2	-1.2625	2.0084	-1.5379	1.4949	2.4722	-1.9054	0.64216	3.9394	-
Node 3	-2.9143	-1.1867	0.58662	1.6268	-1.995	2.3412	-0.6328	2.946	-
Node 4	-1.35	1.489	-1.8677	-1.5295	-1.585	-2.9664	-1.0239	2.2105	-
Node 5	2.5372	-0.0875	-2.057	-1.2016	0.35133	3.1498	-1.8568	-0.8106	-
Node 6	0.25862	1.3789	1.7669	-2.1967	-0.1888	-2.995	-1.5746	-0.5444	-
Node 7	-0.1379	2.4461	0.26625	-0.4596	1.7655	2.8143	1.3585	0.37002	-
Node 8	-1.0545	-0.0605	2.9446	2.8226	0.15898	-1.5928	-0.1011	-0.1590	-
Node 9	1.6029	2.1827	-3.1115	0.27195	-1.6601	0.30525	0.87172	-0.4882	-
Node 10	1.9747	-1.9675	-0.3196	1.3692	1.7427	2.9141	0.98504	1.1482	-
Node 11	-0.0468	2.1972	0.13591	1.1114	-2.6795	2.7945	0.96851	1.1291	-
Node 12	-2.1131	-2.6384	1.1274	1.1272	1.3603	-1.8536	-1.8381	0.7921	-
Node 13	-0.5279	-0.3021	2.724	2.9029	1.2099	1.3633	-2.6271	0.80781	-
Node 14	0.0365	-2.7636	-1.7993	0.91934	-1.4456	2.4717	0.1776	3.0041	-
Node 15	-0.9784	1.9368	-0.7579	-1.8431	-1.362	2.8226	-0.2872	-3.9263	-
Node 16	-0.1474	-1.7758	-2.8125	0.3824	-1.9395	-2.2417	0.0681	-4.4138	-
Output	-	-	-	-	-	-	-	-	-0.2269

Figure 1. *R*-values vs the different number of hidden nodes.

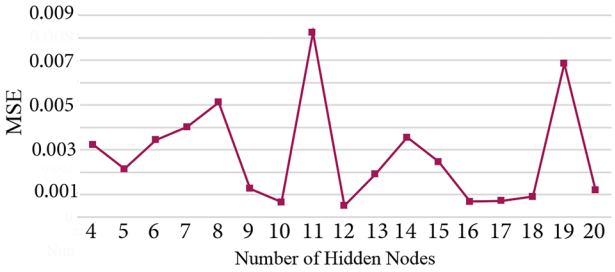

Figure 2. MSE versus hidden nodes number.

Network with 16 nodes of the hidden layer was chosen since it presents good results in the case of *R*-values and also has the least value of MSE among all networks. The results for training are summarized in Figures 3–5.

6. Sensitivity analysis

To calculate the influence of the input data on the effective moment of inertia has used the weight matrix according to Table 4 and the equation of Milne [54]. This study used the modified version of Grason's equation [55] because it considers

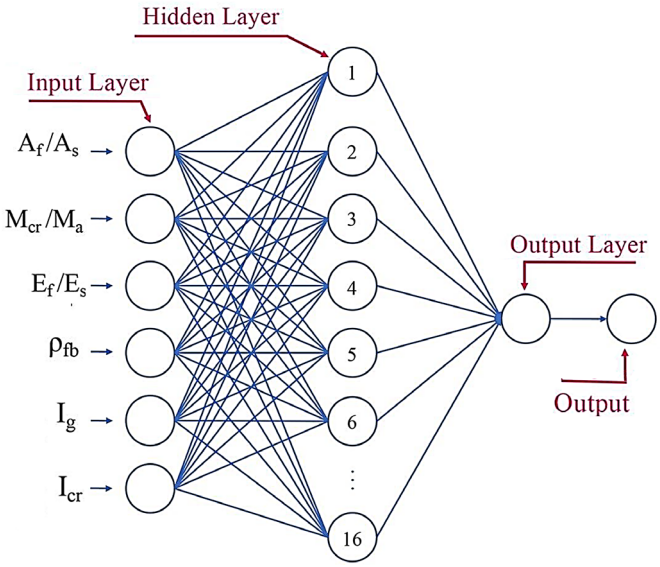

Figure 3. Scheme of ANN.

the absolute values of weights. Milne's formula is presented in Eq. (16):

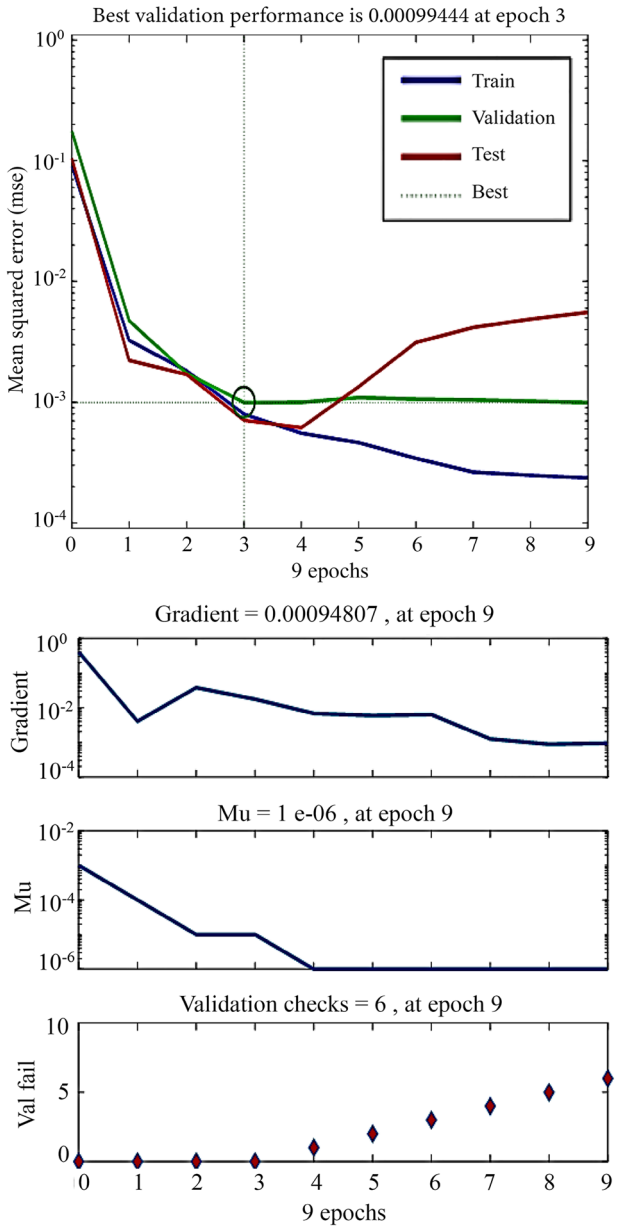

Figure 4. Performance and Training state of ANN.

$$\frac{\sum_{j=1}^{\text{nhidden}} \frac{w_{ji}}{\sum_{l=1}^{\text{ninputs}} |w_{jl}|} . w_{oj}}{\sum_{k=1}^{\text{ninputs}} \left(\sum_{j=1}^{\text{nhidden}} \left| \frac{w_{jk}}{\sum_{l=1}^{\text{ninputs}} |w_{jl}|} . w_{oj} \right| \right)}, \tag{16}$$

where w_{jl} and w_{oj} are the weight between neuron j in the hidden layer with input Node 1 and the weight between neuron j and neuron o in the output layer, respectively.

In Figure 6, the percentage influence of each of the six input parameters on the effective moment of inertia is shown. Table 4 presents the details of weights and their bias of the proposed NN.

7. Proposed approach

The range and the reference value of the six inputs data are represented in Table 5. The reference numbers were considered close to the mean values. As the first step, I_e is plotted against ρ_{fb} while the other input parameters have the reference values, as shown in Figure 7. To account for the

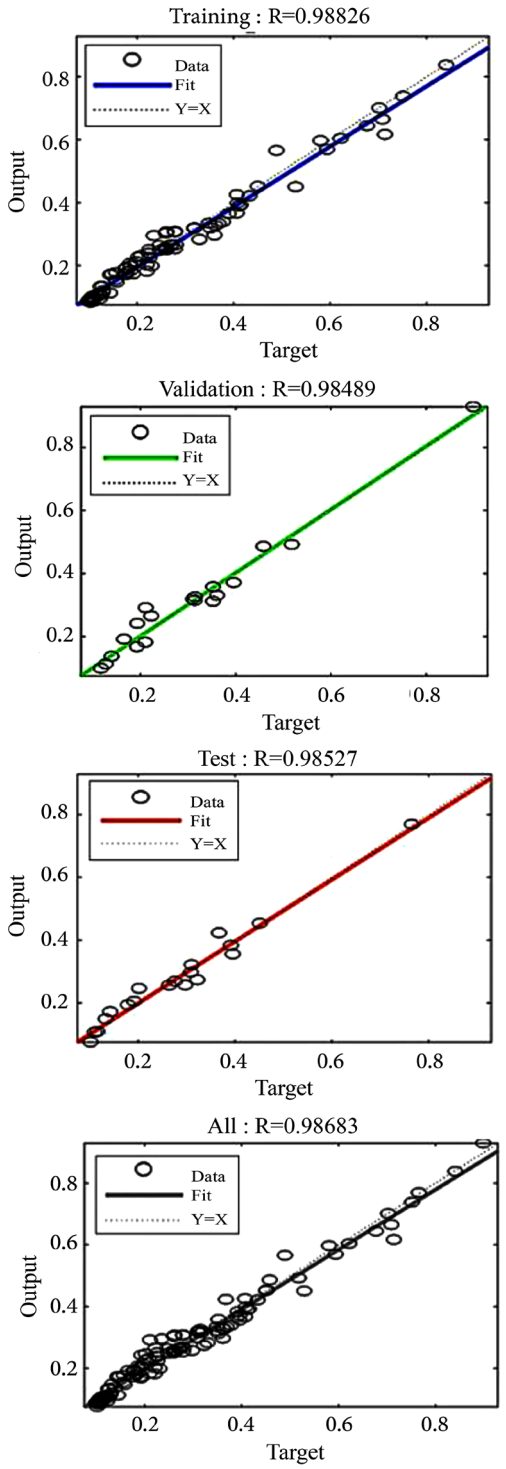

Figure 5. Regressions of training, validation, and test data simulated by ANN.

Table 5. The input parameters range and reference values.

Input parameters	Minimum	Maximum	Reference
I_g (mm^4)	6.67E+7	5.18E+8	2.7E+8
A_f/A_s	0.25	2.88	1.2
M_{cr}/M_a	0.11	0.99	0.40
E_f/E_s	0.19	0.73	0.45
I_{cr} (mm^4)	1.57E+7	1.62E+8	6.9E+7
ρ_{fb}	0.0013	0.0073	0.004

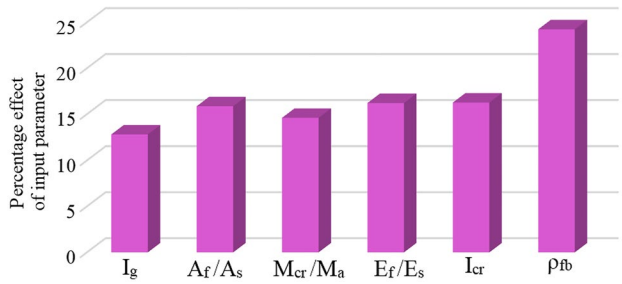

Figure 6. Contribution of input parameters in target.

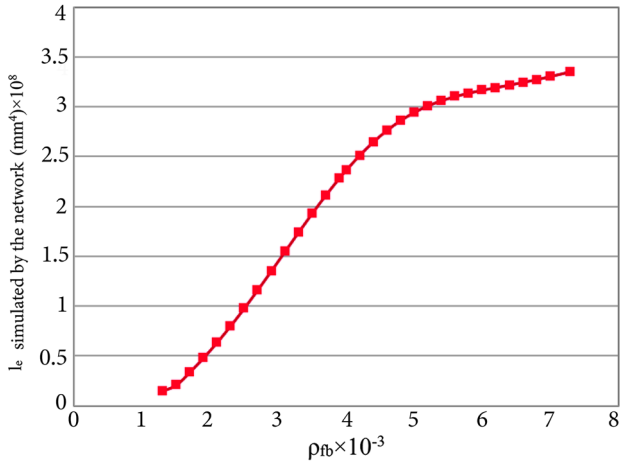

Figure 7. Variation of I_e against ρ_{fb}.

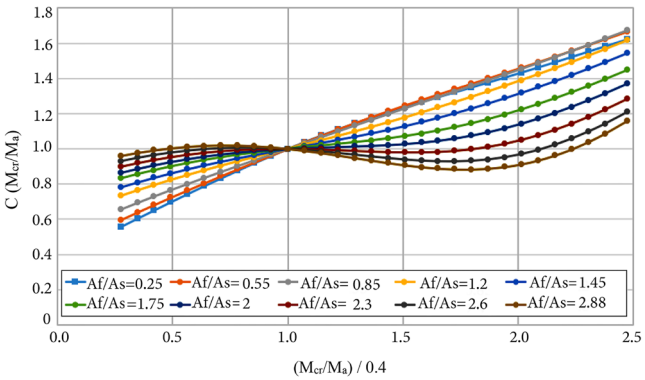

Figure 8. Factor $C\ (M_{cr}/M_a)$ for different (A_f/A_s) values.

effect of other factors on I_e, the correction function can be computed from Eq. (17).

$$F\left(\frac{M_{cr}}{M_a},\frac{A_f}{A_s},I_g,\frac{E_f}{E_s},I_{cr}\right)=C\left(\frac{M_{cr}}{M_a}\right)\times C\left(\frac{A_f}{A_s}\right)\times C\left(I_g\right)\times C\left(\frac{E_f}{E_s}\right)\times C\left(I_{cr}\right). \quad (17)$$

To draw a curve in Figure 8, reference values are considered for the input parameters except for A_f/A_s and M_{cr}/M_a. For A_f/A_s one of the values specified in the figure and for M_{cr}/M_a the entire data range is applied as input. To determine $C\ (M_{cr}/M_a)$, the result obtained I_e from the above NN divided by the value in the case where M_{cr}/M_a also has a reference value. Another 9 curves are plotted in the figure with the same method and various values of A_f/A_s. A similar method was applied to draw $C(M_{cr}/M_a)$ versus other input parameters including

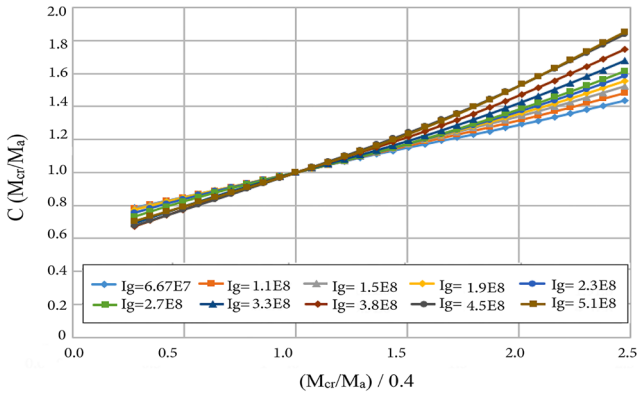

Figure 9. Factor $C\ (M_{cr}/M_a)$ for different I_g values.

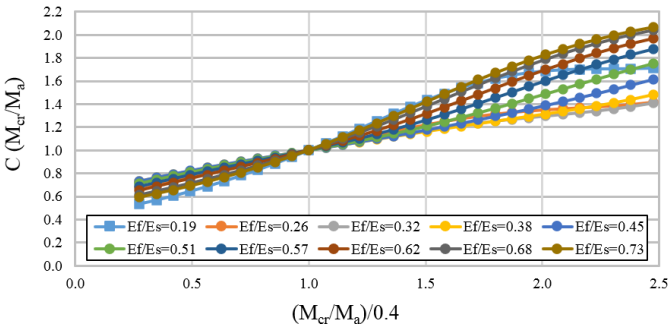

Figure 10. Factor C (M_{cr}/M_a) for different (E_f/E_s) values.

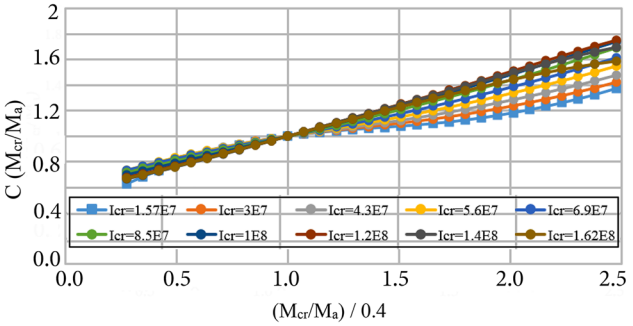

Figure 11. Factor $C\ (M_{cr}/M_a)$ for different I_{cr} values.

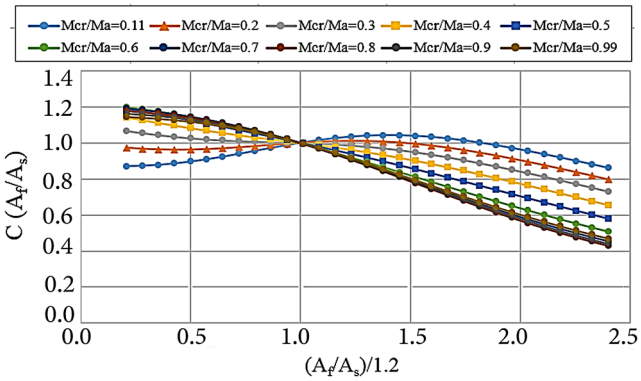

Figure 12. Factor $C\ (A_f/A_s)$ for different (M_{cr}/M_a) values.

I_g, E_f/E_s, and I_{cr} (Figures 9-11). The same method has been utilized to achieve the correction factors for the other input parameters. Some of them are exhibited in Figures 12–15.

To determine the following Eqs. (18)–(22), according to 40 curves related to each correction factor, a line with the least squared error was drawn and the corresponding equations were presented:

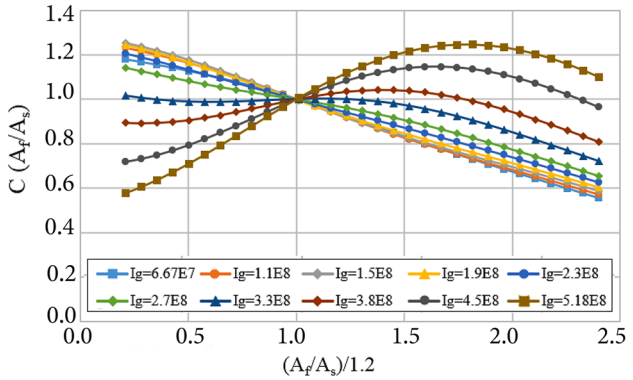

Figure 13. Factor *C (Af/As)* for different I_g values.

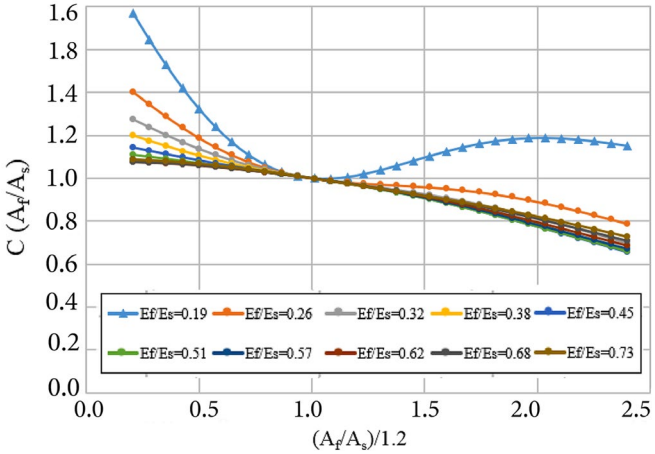

Figure 14. Factor *C (Af/As)* for different (E_f/E_a) values.

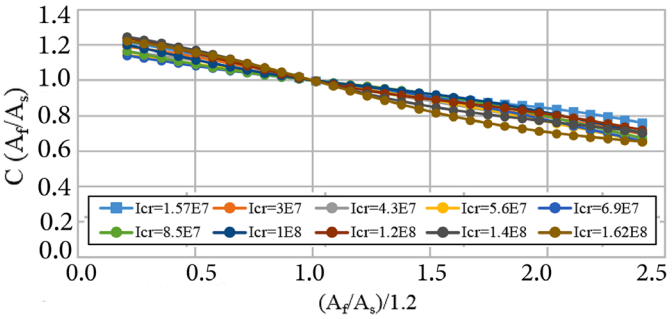

Figure 15. Factor *C (Af/As)* for different I_{cr} values.

$$C\left(\frac{M_{cr}}{M_a}\right)=0.37\times\left(\frac{M_{cr}/M_a}{0.4}\right)+0.63, \tag{18}$$

$$C\left(\frac{A_f}{A_s}\right)=-0.2\times\left(\frac{A_f/A_s}{1.2}\right)+1.2, \tag{19}$$

$$C(I_g)=-0.095\times\ln\left(\frac{I_g}{2.7E+8}\right)+0.99, \tag{20}$$

$$C\left(\frac{E_f}{E_s}\right)=0.87\times\ln\left(\frac{E_f/E_s}{0.45}\right)+1, \tag{21}$$

$$C(I_{cr})=-0.03\left(\frac{I_{cr}}{6.9E+7}\right)^2+0.44\left(\frac{I_{cr}}{6.9E+7}\right)+0.56. \tag{22}$$

Consequently, the effective moment of inertia will be established from Eq. (23) in which, (I_e) curve can be read from Figure 7.

$$I_e=(I_e)_{\text{curve}}\times C\left(\frac{M_{cr}}{M_a}\right)\times C\left(\frac{A_f}{A_s}\right)\times C(I_g)\times C\left(\frac{E_f}{E_s}\right)\times C(I_{cr}). \tag{23}$$

8. Neuro-fuzzy approach

The neuro-fuzzy model defined in this article has five Gaussian membership functions for each input variable. Each membership function represents a language expression for the variable. For example, membership function number 1 represents very low values and membership function number 5 represents very high values. Each of the above Gaussian functions, also shown in Figure 16, has two parameters, including the mean value *m* as well as the value of variance *v*, the details of which can be seen in Table 6.

In adjusting the structure of the above system (Figure 17), five fuzzy rules are considered, which will be used to estimate the output parameter. Using the data used in the NN training process, the best neuro-fuzzy model was determined, the results of training and test datasets can be seen in Figure 18.

As shown in Figure 17, the proposed model has five linear functions. These functions ($F_1, \ldots, F_5$), which include a set of coefficients for each of the input variables and a constant, are shown in Eqs. (24) to (28). The above coefficients (Table 7) are determined by the neuro-fuzzy optimization algorithm in the training process of the model.

$$F_1=-2.13X_1-0.51X_2+1.92X_3+0.99X_4+1.848X_5+1.55X_6-0.9, \tag{24}$$

$$F_2=-1.97X_1-25.33X_2+0.94X_3-11.74X_4-0.49X_5+15.01X_6-3.33, \tag{25}$$

$$F_3=-1.75X_1+0.08X_2+0.33X_3-0.6X_4+0.63X_5+2.29X_6+0.58, \tag{26}$$

$$F_4=-0.06X_1+0.01X_2+0.27X_3+3.53X_4-0.27X_5-0.08X_6-0.17, \tag{27}$$

$$F_5=3.89X_1-0.16X_2+0.11X_3+6.13X_4-0.16X_5-0.06X_6-1.63. \tag{28}$$

Using the number of input variables, the value of each of the linear functions is determined. Then, the value of the output variable is estimated by Eq. (29). It should be noted that the output value obtained by this equation is normalized and needs to be converted to its real value by the relation provided in Table 3.

$$0.1\le\left(Y=\frac{\sum_{i=1}^{5}G_iW_i}{\sum_{i=1}^{5}W_i}\right)\le 0.9. \tag{29}$$

The parameter *W* in the above equation is related to the set of fuzzy rules of the system (five rules for the proposed model) whose values can be calculated using Eq. (30) to (34) with consideration of the Gaussian membership functions provided in Table 6.

Table 6. Gaussian membership function details.

Input	Parameter	*G1*	*G2*	*G3*	*G 4*	*G5*
X1	*v*	0.0991	0.0905	0.1769	0.1075	0.1155
	m	0.4045	0.4078	0.8869	0.3711	0.1633
X2	*v*	0.0937	0.0954	0.1111	0.0880	0.0909
	m	0.2060	0.1333	0.5358	0.4446	0.3482
X3	*v*	0.0891	0.0830	0.0858	0.0816	0.1131
	m	0.2501	0.2850	0.4449	0.3473	0.5661
X4	*v*	0.02465	0.0203	0.01689	0.02401	0.01897
	m	0.1368	0.1287	0.1907	0.1236	0.1865
X5	*v*	0.1133	0.1930	0.1085	0.1076	0.1194
	m	0.5207	0.8828	0.4896	0.2751	0.1331
X6	*v*	0.0723	0.0906	0.0563	0.0796	0.1350
	m	0.5041	0.6325	0.4078	0.5381	0.1518

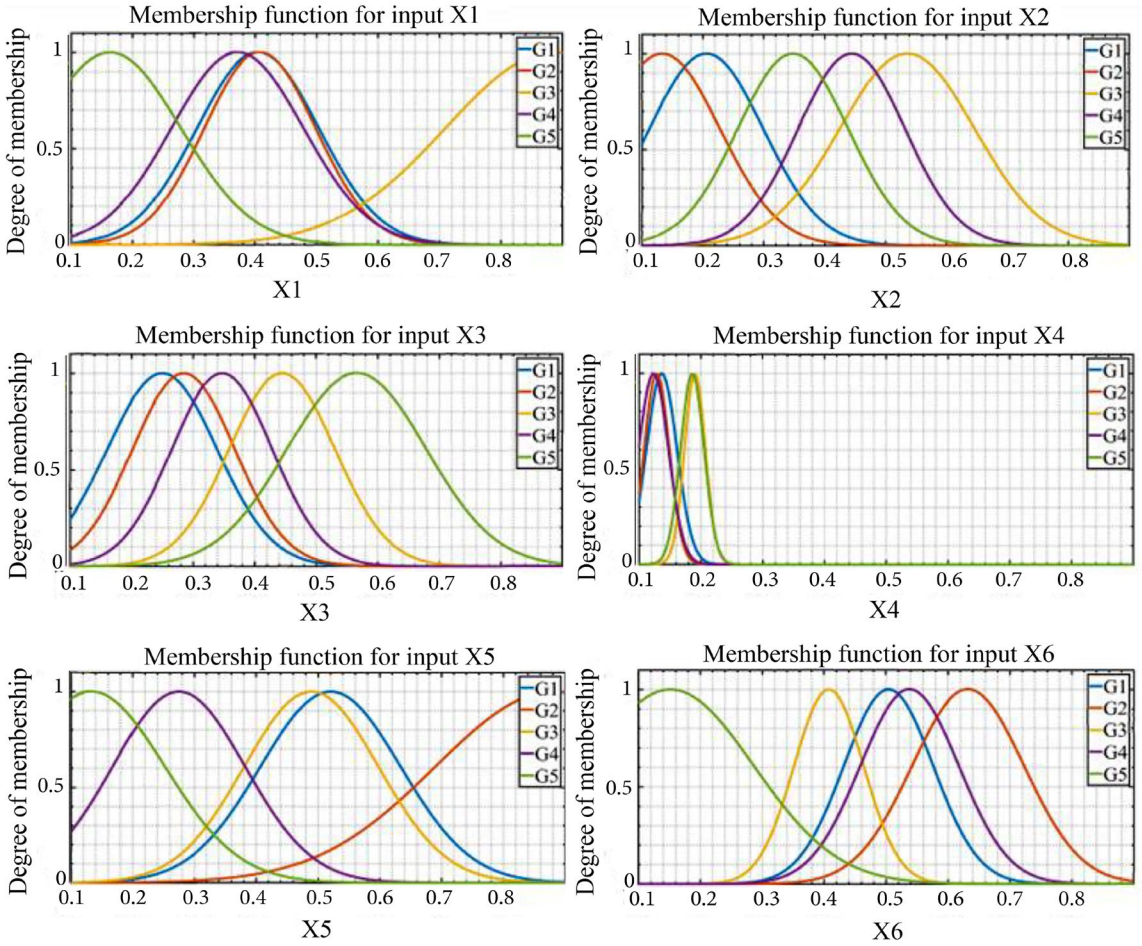

Figure 16. Gaussian membership functions for the considered inputs.

Table 7. Output functions.

Input	*F1*	*F2*	*F3*	*F4*	*F 5*
X1	-2.1300	-1.9720	-1.7470	-0.0629	3.8920
X2	-0.5103	-25.3300	0.0860	0.0172	-0.1555
X3	1.9180	0.9402	0.3254	0.2661	0.1091
X4	0.9948	-11.7400	-0.6004	3.5290	6.1320
X5	1.8480	-0.4929	0.6282	-0.2726	-0.1599
X6	1.5500	15.0100	2.2860	-0.0850	-0.0603
Constant	-0.8997	-3.3320	0.5812	-0.1729	-1.6260

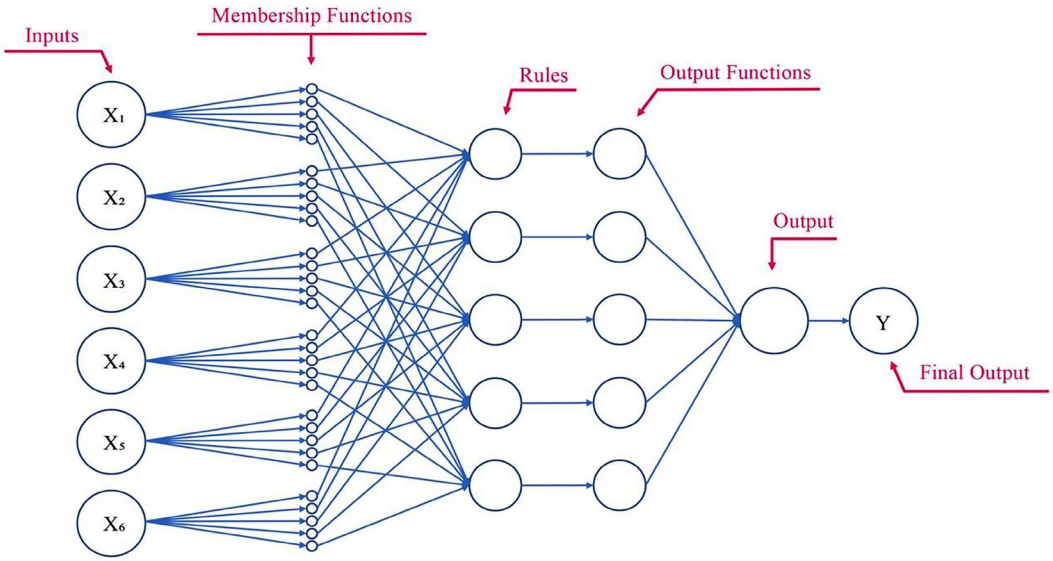

Figure 17. Proposed ANFIS structure.

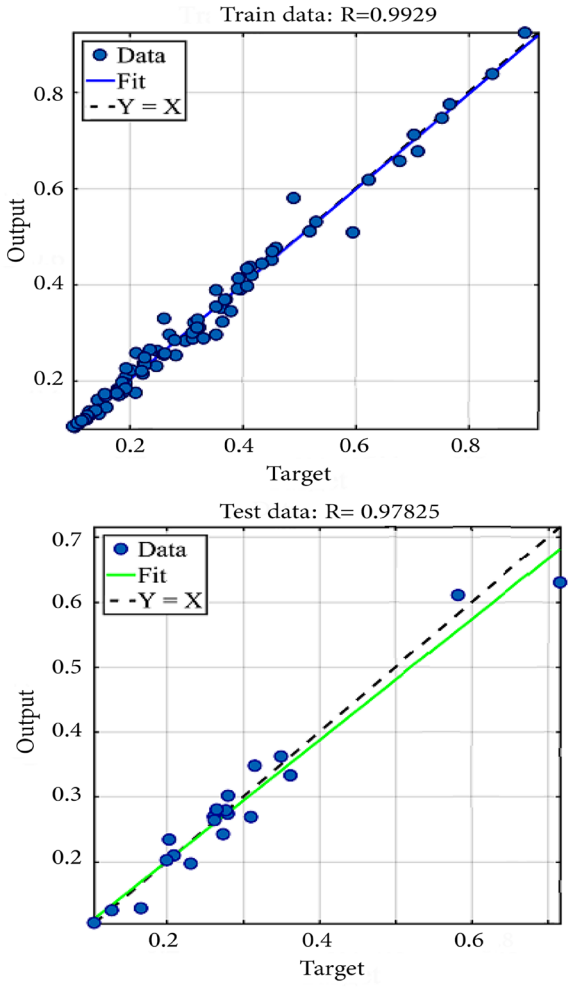

Figure 18. Regression plots obtained from ANFIS.

$$W_1 = G_{1,X1}\, G_{1,X2}\, G_{1,X3}\, G_{1,X4}\, G_{1,X5}\, G_{1,X6}, \quad (30)$$

$$W_2 = G_{2,X1}\, G_{2,X2}\, G_{2,X3}\, G_{2,X4}\, G_{2,X5}\, G_{2,X6}, \quad (31)$$

$$W_3 = G_{3,X1}\, G_{3,X2}\, G_{3,X3}\, G_{3,X4}\, G_{3,X5}\, G_{3,X6}, \quad (32)$$

$$W_4 = G_{4,X1}\, G_{4,X2}\, G_{4,X3}\, G_{4,X4}\, G_{4,X5}\, G_{4,X6}, \quad (33)$$

$$W_5 = G_{5,X1}\, G_{5,X2}\, G_{5,X3}\, G_{5,X4}\, G_{5,X5}\, G_{5,X6}. \quad (34)$$

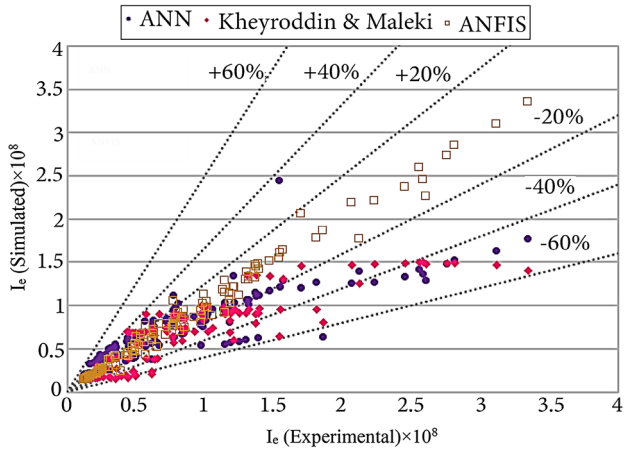

Figure 19. Comparison of predicted values of I_e between the proposed equations and equation using GA.

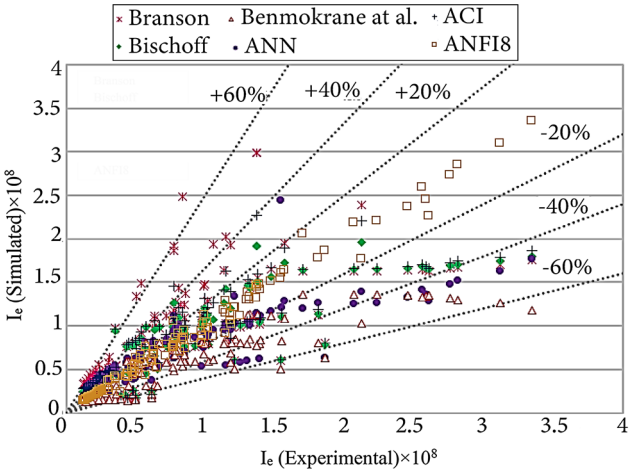

Figure 20. Comparison of predicted values of I_e between the proposed equations and six existing equations.

9. Comparison study

To verify the proposed ANN and ANFIS models compared with the GA method and existing models, respectively, Figures 19 and 20 have been presented. Also, the distribution

Table 8. The errors range for various existing equations versus the ANN and ANFIS models.

Range of error (%)	Branson	Bischoff	ACI	ANN model	Benmokrane et al.	ANFIS model
±15	16	33	25	34	31	107
±30	37	74	61	85	63	121
±45	81	107	104	111	92	122
±60	110	117	119	121	114	122
±75	122	122	122	122	122	122

Table 9. The percentage errors for various existing equations versus the ANN and ANFIS models.

Range of error (%)	Branson (%)	Bischoff (%)	ACI (%)	ANN model (%)	Benmokrane et al. (%)	ANFIS model (%)
±15	13.11	27.05	20.49	27.87	25.41	87.70
±30	30.33	60.66	50	69.67	51.64	99.18
±45	66.39	87.70	85.25	90.98	75.41	100
±60	90.16	95.90	97.54	99.18	93.44	100
±75	100	100	100	100	100	100

Table 10. Comparison of average error of I_e between the proposed equation and four existing models.

Average error	Branson	Bischoff	ACI	ANN model	Benmokrane et al.	ANFIS model
	62.08	34.64	43.46	30.28	31.24	7.59

of error and percentage error for various equations is shown in Tables 8 and 9, respectively.

At first, the error value of existing and proposed models is calculated from Eq. (35) then the calculating average error is presented in Table 10.

$$e = \left| \frac{(I_e)_{\text{theo}} - (I_e)_{\text{exp}}}{(I_e)_{\text{exp}}} \right| \times 100. \quad (35)$$

According to the results of the proposed methods and their comparison with existing methods, it can be seen that the use of ANFIS and ANN models have higher accuracy and lower error percentage in estimating the effective moment of inertia. The proposed equation using the ANN method reduces the error in the calculation of I_e by about 51.22, 17.36, 30.33, and 3.07 percent, compared with the equations proposed by Branson, Bischoff, ACI, and Benmokrane, respectively. Also, this error reduction in the proposed equation with ANFIS is 87.77, 79.28, 82.54, and 75.70 percent respectively.

10. Conclusions

A wide number of experimental data for hybrid Reinforced Concrete (RC) beams was collected. To predict the effective moment of inertia using the Neural Network (NN), six related parameters were considered as network inputs. After investigating the performance (R and Mean Square Error (MSE)) of 17 NNs with various numbers of nodes in the hidden layer, a network with the highest performance in the simulation was chosen. According to these correction coefficients obtained from the simulated results of the NN, a general equation was presented to calculate I_e in hybrid beams independent of the NN. The average error of the proposed model is 30%, and more than 99% simulated result is within a 60% range of error. A comparison of the results from Artificial Neural Networks (ANN) simulation, Adaptive Neural Fuzzy Inference System (ANFIS) model, and available equations with the experimental data showed that the Soft Computing (SC) models have high accuracy. The precision of the ANN and ANFIS models was verified by existing experimental data and exhibited good agreement. Also, the comparison of two SC models revealed that the ANFIS model is less error and more accurate than ANN in predicting I_e in hybrid beams.

Funding

This research did not receive any specific grant from funding agencies in the public, commercial, or not-forprofit sectors.

Conflicts of interest

The authors declare that they have no known competing financial interests or personal relationships that could have appeared to influence the work reported in this paper.

Authors contribution statement

First author

Fahimeh Maleki: Data curation; Methodology; Formal analysis; Investigation; Project administration; Resources; Software; Validation; Writing – original draft

Second author

Ali Kheyroddin**:** Conceptualization; Methodology; Project administration; Supervision; Writing – review & editing

Third author

Hosein Naderpour: Conceptualization; Methodology; Writing – review & editing

Fourth author

Masoomeh Mirrashid: Software; Writing – review & editing.

References

1. Dundar, C., Tanrikulu, A.K., and Frosch, R.J. "Prediction of load–deflection behavior of multi-span FRP and steel reinforced concrete beams", *Composite Structures*, **132**, pp. 680-693 (2015). https://doi.org/10.1016/j.compstruct.2015.06.018

2. Tan, K. "Behaviour of hybrid FRP-steel reinforced concrete beams", In *Proc., 3rd Int. Symposium,* FRPRCS (1997).

3. Qin, R., Zhou, A., and Lau, D., "Effect of reinforcement ratio on the flexural performance of hybrid FRP reinforced concrete beams", *Composites Part B: Engineering*, **108**, pp. 200-209 (2017). https://doi.org/10.1016/j.compositesb.2016.09.054

4. Akiel, M.S., El-Maaddawy, T., and El Refai, A. "Serviceability and moment redistribution of continuous concrete members reinforced with hybrid steel-BFRP bars", *Construction and Building Materials*, **175**, pp. 672-681 (2018). https://doi.org/10.1016/j.conbuildmat.2018.04.202

5. Sheikh, S.A. and Kharal, Z. "Replacement of steel with GFRP for sustainable reinforced concrete", *Construction and Building Materials*, **160**, pp. 767-774 (2018). https://doi.org/10.1016/j.conbuildmat.2017.12.141

6. Salleh, N., Hamid, N.A., and Majid, M.A. "Finite element modelling of concrete beams reinforced with hybrid fiber reinforced bars". In *IOP Conference Series: Materials Science and Engineering*. IOP Publishing (2017).

7. Pang, L., Qu, W., Zhu, P., et al. "Design propositions for hybrid FRP-steel reinforced concrete beams", *Journal of Composites for Construction*, **20**(4), 04015086 (2016). https://doi.org/10.1061/(ASCE)CC.1943-5614.0000654

8. El Refai, A., Abed, F., and Al-Rahmani, A. "Structural performance and serviceability of concrete beams reinforced with hybrid (GFRP and steel) bars", *Construction and Building Materials*, **96**, pp. 518-529 (2015). https://doi.org/10.1016/j.conbuildmat.2015.08.063

9. Kara, I.F., Ashour, A.F., and Köroğlu, M.A. "Flexural behavior of hybrid FRP/steel reinforced concrete beams", *Composite Structures*, **129**, pp. 111-121 (2015). https://doi.org/10.1016/j.compstruct.2015.03.073

10. Al-Sunna, R., Pilakoutas, K., Hajirasouliha, I., et al. "Deflection behaviour of FRP reinforced concrete beams and slabs: An experimental investigation", *Composites Part B: Engineering*, **43**(5), pp. 2125-2134 (2012). https://doi.org/10.1016/j.compositesb.2012.03.007

11. Naderpour, H., Kheyroddin, A., and Amiri, G.G., "Prediction of FRP-confined compressive strength of concrete using artificial neural networks", *Composite Structures*, **92**(12), pp. 2817-2829 (2010). https://doi.org/10.1016/j.compstruct.2010.04.008

12. Kheyroddin, A., *Nonlinear Finite Element Analysis of Flexure-Dominant Reinforced Concrete Structures*, McGill University Canada (1996).

13. Kheyroddin, A. and Mirza, M. "Flexural rigidity of reinforced concrete beams", In *Canadian Society for Civil Engineering Annual Conference Proceedings,* June (1995).

14. Bui, L.V.H., Stitmannaithum, B., and Ueda, T. "Ductility of concrete beams reinforced with both fiber-reinforced polymer and steel tension bars", *Journal of Advanced Concrete Technology*, **16**(11), pp. 531-548 (2018). https://doi.org/10.3151/jact.16.531

15. Shield, C., Brown, V., Bakis, C.E., et al. "A Recalibration of the Crack Width Bond-Dependent Coefficient for GFRP-Reinforced Concrete", *Journal of Composites for Construction*, **23**(4), 04019020 (2019). https://doi.org/10.1061/(ASCE)CC.1943-5614.0000978

16. Nguyen, H.D., Zhang, Q., Choi, E., et al. "An improved deflection model for FRP RC beams using an artificial intelligence-based approach", *Engineering Structures*, **219**, 110793 (2020). https://doi.org/10.1016/j.engstruct.2020.110793

17. Ge, W., Wang, Y., Ashour, A., et al. "Flexural performance of concrete beams reinforced with steel–FRP composite bars", *Archives of Civil and Mechanical Engineering*, **20**(2), p. 56 (2020). https://doi.org/10.1007/s43452-020-00058-6

18. Moolaei, S., Sharbatdar, M.K., and Kheyroddin, A. "Experimental evaluation of flexural behavior of HPFRCC beams reinforced with hybrid steel and GFRP bars", *Composite Structures*, **275**, 114503 (2021). https://doi.org/10.1016/j.compstruct.2021.114503

19. Wang, X., Liu, S., Shi, Y., et al. "Integrated High-Performance Concrete Beams Reinforced with Hybrid BFRP and Steel Bars", *Journal of Structural Engineering*, **148**(1), 04021235 (2022). https://doi.org/10.1061/(ASCE)ST.1943541X.0003207

20. Arabshahi, A., Tavakol, M., Sabzi, J., et al. "Prediction of the effective moment of inertia for concrete beams reinforced with FRP bars using an evolutionary algorithm", In *Structures*. Elsevier (2022).

21. Lyu, Z., Yu, Y., Samali, B., et al. "Back-propagation neural network optimized by K-fold cross-validation for prediction of torsional strength of reinforced Concrete beam", *Materials*, **15**(4), 1477 (2022). https://doi.org/10.3390/ma15041477

22. Li, N., Asteris, P.G., Tran, T.-T., et al. "Modelling the deflection of reinforced concrete beams using the improved artificial neural network by imperialist competitive optimization", *Steel and Composite Structures*, **42**(6), pp. 733-745 (2022). https://doi.org/10.12989/scs.2022.42.6.733

23. Jayasinghe, T., Gunawardena, T., and Mendis, P. "Assessment of shear strength of reinforced concrete beams without shear reinforcement: A comparative study between codes of practice and artificial neural network", *Case Studies in Construction Materials*, **16**, e01102 (2022). https://doi.org/10.1016/j.cscm.2022.e01102

24. Alagundi, S. and Palanisamy, T. "Neural network prediction of joint shear strength of exterior beam-column joint", In *Structures*, Elsevier (2022).

25. Zayan, H.S. and Mahmoud, A.S. "Estimations the combined flexural-torsional strength for prestressed concrete beams using artificial neural networks", In *Geotechnical Engineering and Sustainable Construction*, Springer, pp. 583-596 (2022).

26. Zhang, P., Fan, W., Chen, Y., et al. "Structural symmetry recognition in planar structures using Convolutional Neural Networks", *Engineering Structures*, **260**, 114227 (2022). https://doi.org/10.1016/j.engstruct.2022.114227

27. Khan, K., Iqbal, M., Salami, B.A., et al. "Estimating flexural strength of FRP reinforced beam using artificial neural network and random forest prediction models", *Polymers*, **14**(11), 2270 (2022). https://doi.org/10.3390/polym14112270

28. Peng, J., Yan, G., Zandi, Y., et al. "Prediction and optimization of the flexural behavior of corroded concrete beams using adaptive neuro fuzzy inference system", In *Structures*, Elsevier (2022).

29. Barkhordari, M.S., Feng, D.-C., and Tehranizadeh, M., "Efficiency of hybrid algorithms for estimating the shear strength of deep reinforced concrete beams", *Periodica Polytechnica Civil Engineering*, **66**(2), pp. 398-410 (2022). https://doi.org/10.3311/PPci.19323

30. Fan, W., Chen, Y., Li, J., et al. "Machine learning applied to the design and inspection of reinforced concrete bridges: Resilient methods and emerging applications", In *Structures*. Elsevier (2021).

31. Buyukkaragoz, A., Kalkan, I., and Lee, J. "A numerical study of the flexural behavior of concrete beams reinforced with AFRP bars", *Strength of Materials*, **45**(6), pp. 716-729 (2013). https://doi.org/10.1007/s11223-013-9507-5

32. Chen, Y., Feng, J., and Yin, S. "Compressive behavior of reinforced concrete columns confined by multi-spiral hoops", *Computers and concrete*, **9**(5), pp. 341-355 (2012). https://doi.org/10.12989/cac.2012.9.5.341

33. Patel, K., Bhardwaj, A., Chaudhary, S., et al. "Explicit expression for effective moment of inertia of RC beams", *Latin American Journal of Solids and Structures*, **12**(3), pp. 542-560 (2015). http://dx.doi.org/10.1590/1679-78251272

34. ACI, Guide for the Design and Construction of Structural Concrete Reinforced with FRP Bars (ACI 440.1 R-15), American Concrete Institute (2015).

35. Pirayeh Gar, S., Mander, J.B., and Hurlebaus, S. "Deflection of FRP prestressed concrete beams", *Journal of Composites for Construction*, **22**(2), 04017049 (2018). https://doi.org/10.1061/(ASCE)CC.1943-5614.0000832

36. Branson, D.E. "Design procedures for computing deflections". In *Journal Proceedings,* **65**(9), pp. 730-742 (1968).

37. Benmokrane, B. and Masmoudi, R. "Flexural response of concrete beams reinforced with FRP reinforcing bars", *Structural Journal*, **93**(1), pp. 46-55 (1996).

38. Masmoudi, R. "Theoretical and experimental evaluation of the flexural behaviour of beams reinforced with FRP rebars", Doctoral Thesis, Department of Civil Engineering, University de Sherbrooke, Sherbrooke, Canada, **19**, p. 273 (1996).

39. Masmoudi, R., Theriault, M., and Benmokrane, B. "Flexural Behavior of Concrete Beams Reinforced with FRP C-BAR Reinforcing Rods", *Tech. Rep. 2 Submitted to Marshall Industries Composites*, Inc (1996).

40. Yost, J.R., Gross, S.P., and Dinehart, D.W. "Effective moment of inertia for glass fiber-reinforced polymer-reinforced concrete beams", *Structural Journal*, **100**(6), pp. 732-739 (2003).

41. Bischoff, P.H. "Deflection calculation of FRP reinforced concrete beams based on modifications to the existing Branson equation", *Journal of Composites for Construction*, **11**(1), pp. 4-14 (2007). https://doi.org/10.1061/(ASCE)1090-0268(2007)11:1(4)

42. Bischoff, P., Gross, S., and Ospina, C. "The story behind proposed changes to ACI 440 deflection requirements for FRP-reinforced concrete", *Special Publication*, **264**, pp. 53-76 (2009).

43. Mousavi, S.R. and Esfahani, M.R. "Effective moment of inertia prediction of FRP-reinforced concrete beams based on experimental results", *Journal of Composites for Construction*, 16(5), pp. 490-498 (2012). https://doi.org/10.1061/(ASCE)CC.1943-5614.0000284

44. Kheyroddin, A. and Maleki, F., "Prediction of effective moment of inertia for hybrid FRP-steel reinforced concrete beams using the genetic algorithm", *Journal of Numerical Methods in Civil Engineering*, **2**(1), pp. 15-23 (2017) https://doi.org/10.29252/nmce.2.1.15

45. Zadeh, L.A. "Fuzzy logic, neural networks, and soft computing", In *Fuzzy Sets, Fuzzy Logic, And Fuzzy Systems: Selected Papers by Lotfi A Zadeh*, World Scientific, pp. 775-782 (1996).

46. Ross, T.J., *Fuzzy Logic with Engineering Applications*, John Wiley & Sons, Ltd. ISBN: 978-0-470-74376-8 (2010).

47. Chalabi, M., Naderpour, H., and Mirrashid, M. "Seismic resilience index for RC moment frames of school buildings using neuro-fuzzy approach", *Natural Hazards*, pp. 1-26 (2022). https://doi.org/10.1007/s11069-022-05377-w

48. Mirrashid, M. and Naderpour, H. "Recent trends in prediction of concrete elements behavior using soft computing (2010–2020)", *Archives of Computational Methods in Engineering*, **28**(4), pp. 3307-3327 (2021). https://doi.org/10.1007/s11831-020-09500-7

49. Mirrashid, M. and Naderpour, H. "Computational intelligence-based models for estimating the fundamental period of infilled reinforced concrete frames", *Journal of Building Engineering*, **46**, 103456 (2022). https://doi.org/10.1016/j.jobe.2021.103456

50. Naderpour, H., Akbari, M., Mirrashid, M., et al. "Compressive Capacity Prediction of Stirrup-Confined Concrete Columns Using Neuro-Fuzzy System", *Buildings*, **12**(9), p. 1386 (2022). https://doi.org/10.3390/buildings12091386

51. Naderpour, H., Haji, M., and Mirrashid, M. "Shear capacity estimation of FRP-reinforced concrete beams using computational intelligence", In *Structures*, Elsevier (2020).

52. Naderpour, H., Mirrashid, M., and Parsa, P., "Failure mode prediction of reinforced concrete columns using machine learning methods", *Engineering Structures*, **248**, 113263 (2021). https://doi.org/10.1016/j.engstruct.2021.113263

53. Jang, J.-S. "ANFIS: adaptive-network-based fuzzy inference system", *IEEE Transactions on Systems, Man, and Cybernetics*, **23**(3), pp. 665-685 (1993). https://doi.org/10.1109/21.256541

54. Milne, L. "Feature selection using neural networks with contribution measures", In *AI-CONFERENCE-*. Citeseer (1995).

55. Pentoś, K., Łuczycka, D., and Kapłon, T. "The identification of relationships between selected honey parameters by extracting the contribution of independent variables in a neural network model", *European Food Research and Technology,* **241**(6), pp. 793-801 (2015). https://doi.org/10.1007/s00217-015-2504-0

56. Aiello, M.A. and Ombres, L. "Structural performances of concrete beams with hybrid (fiber-reinforced polymer-steel) reinforcements", *Journal of Composites for Construction*, **6**(2), pp. 133-140 (2002). https://doi.org/10.1061/(ASCE)1090-0268(2002)6:2(133

57. Qu, W., Zhang, X., and Huang, H. "Flexural behavior of concrete beams reinforced with hybrid (GFRP and steel) bars", *Journal of Composites for construction*, **13**(5), pp. 350-359 (2009). https://doi.org/10.1061/(ASCE)CC.1943-5614.0000035

58. Leung, H.Y. and Balendran, R. "Flexural behaviour of concrete beams internally reinforced with GFRP rods and steel rebars", *Structural Survey*, **21**(4), pp. 146-157 (2003). https://doi.org/10.1108/02630800310507159

59. Almusallam, T.H., Elsanadedy, H.M., Al-Salloum, Y.A., et al., "Experimental and numerical investigation for the flexural strengthening of RC beams using near-surface mounted steel or GFRP bars", *Construction and Building Materials*, **40**, pp. 145-161 (2013). https://doi.org/10.1016/j.conbuildmat.2012.09.107

60. Safan, M.A. "Flexural Behavior and Design of Steel-GFRP Reinforced Concrete Beams", *ACI Materials Journal*, **110**(6), pp. 677-685 (2013). https://doi.org/10.14359/51686335

61. Yang, J., Min, K., Shin, H., et al. "Behavior of high-strength concrete beams reinforced with different types of flexural reinforcement and fiber", In *Advances in FRP Composites in Civil Engineering*, Springer, pp. 275-278 (2011).

Biographies

Fahimeh Maleki received her BSc and MSc degrees in Civil and Structural Engineering from Semnan University. Now she is a PhD Candidate at Semnan University. She is a member of the Iranian Concrete Institute (ICI). Her study fields include the Finite Element Method, Artificial Neural Networks, Hybrid Concrete Structures, and FRP bars.

Ali Kheyroddin is a Full Professor of Civil Engineering at Semnan University, Iran. He was an Invited Visiting Scholar in the University of Texas at Arlington, Arlington, TX, and he received his MS from Iran University of Science and Technology, Tehran, Iran and his PhD from McGill University, Montreal, QC, Canada .He was the Chancellor of Semnan University for 8 years .His research interests include the analysis and design of reinforced concrete structures, concrete properties, tall buildings, rehabilitation of existing buildings, and design of earthquake-resistant buildings.

Hosein Naderpour received his PhD degree with high honors in Structural Engineering. He then joined Semnan University where he is presently Professor of Structural Engineering. Since joining the faculty of Civil Engineering at Semnan University, Dr. Naderpour has taught a variety of undergraduate and graduate courses in the areas of structural engineering, numerical methods, mechanics of materials, structural stability, concrete structures, structural reliability, as well as soft computing. Dr. Naderpour is author of 60 papers published in journals and about 100 papers presented at national and international conferences. He has given several speeches in Switzerland, China, Australia, South Korea, Romania, Turkey, Canada, Hong Kong, Belgium, Portugal, Spain, Japan, Germany, Italy, Czech Republic and France. He is currently a chief member of Iranian Earthquake Engineering Association, Iran Concrete Institute (ICI), Iranian Society for Light Steel Framing (LSF), Iran's National Elites Foundation, Safe School Committee, Organization for Development, Renovation and Equipping Schools of Iran (DRES). Furthermore, he is currently the editor-in-chief of three international journals in the area of civil and mechanical engineering including Journal of soft computing in Civil Engineering (SCCE), Journal of Computational Engineering and Physical Modeling (CEPM) and Reliability Engineering and Resilience (REngR). His major research interests include: application of soft computing in structural engineering, seismic resilience, structural reliability, structural optimization and damage detection of structures.

Masoomeh Mirrashid is currently postdoctoral research fellow in structural engineering at Semnan University, Iran. She has taught several courses of higher education including theory of elasticity and plasticity, dynamic of structures, advanced concrete and, steel Structures. Her scientific activities include author and co-author of more than twenty ISI articles, technical committee member for more than ten international conferences, editor and, reviewer for international journals. Her fields of interests are structural engineering, earthquake, vulnerability, neural networks, Fuzzy and Neuro-Fuzzy systems, machine learning methods and also optimization algorithms.